Journal of Alloys and Compounds, 189 (1992) 249–258
JALCOM 386

Distribution of carbon atoms on the boron carbide structure elements

U. Kuhlmann and H. Werheit
Solid State Physics Laboratory, University of Duisburg, Lotharstr. 1–21, W-4100 Duisburg 1 (Germany)

K. A. Schwetz
Elektroschmelzwerk Kempten G.m.b.H., W-8960 Kempten (Germany)

(Received June 6, 1992)

Abstract

Optical absorption and reflectivity measurements in the spectral range of the 1580 cm^{-1} phonon, the stretching mode of the central atom of the three-atom chain in the unit cell of boron carbide, were simultaneously fitted by suitable model calculations to determine quantitatively the carbon distribution within the unit cell in the homogeneity range. For example, in $B_{4.3}C$, which is confirmed to be the carbon-rich limit composition, there are 81% C–B–C and 19% C–B–B chains, and exactly one carbon atom substitutes an icosahedral site. The concentrations of the C–B–C and C–B–B chains change abruptly between 11 and 14 at.% C, while the concentration of the carbon atoms in the icosahedra varies non-monotonically. The reduction in the carbon content towards the boron-rich limit of the homogeneity range is accompanied by an increasing number of unit cells without any chains. This number exceeds even 50% at about 8 at.% C. These results allow us to explain easily the variation in several structure and disorder-dependent physical properties of boron carbide and they disprove certain fundamental model assumptions. The force constants of the C–B and B–B bonds in the chain were determined. At $B_{4.3}C$ they have the same value of 5.6(1) mdyn $Å^{-1}$; at lower carbon contents they differ.

1. Introduction

Hitherto boron carbide has been the boron-rich solid which has received the most extensive technical use by far, *e.g.* for grinding and polishing, wear-resistant tools, surface hardening, light weight armour, and high technology ceramics (see refs. 1 and 2, and references therein). Moreover, boron carbide is a very promising material for direct thermoelectric energy conversion (see refs. 3 and 4). Nevertheless, the structural details have not yet been resolved, in particular the distribution of the carbon atoms in the structure, although this distribution has a significant influence on several physical, and especially on the electronic, properties of boron carbide, as is evident from experimental and theoretical investigations [5, 6].

Boron carbide exhibits a large homogeneity range extending from about $B_{4.3}C$ at the carbon-rich to about $B_{12}C$ at the boron-rich limit. Throughout the whole range the structure is single phase consisting of an icosahedral arrangement of twelve atoms at the vertices of the rhombohedral unit cell, and a three-atom chain on its main diagonal, which coincides with the crystallographic *c* axis (Fig. 1) (see ref. 5). The primary structure model of B_4C (according to recent investigations [7], better represented as $B_{4.3}C$), which has been the technically most important chemical composition until now, was based on a (B_{12})C–C–C arrangement, but more recently a $(B_{11}C)$C–B–C arrangement has become favoured. For the structure modifications towards the boron-rich limit of the homogeneity range several models have been discussed: planar B_4 groups [8] or C–B–B chains replacing statistically the carbon-rich chains, and a decreasing substitution of icosahedral sites by carbon atoms. However, all these models were more or less speculative, because the experimental methods hitherto used failed or did not yield unambiguous results [9–12]. Theoretically calculated energies of different structure variants are not significantly different in most cases, and therefore the disregard of additional influences on the energies, *e.g.* the Jahn–Teller effect [13, 14] or the structural reconstruction of the icosahedron in the case of carbon substitution [15], in the calculations makes the validity of such results [16–18] doubtful, particularly when only small energy differences between different structure modifications are obtained.

In this paper a new method to determine the distribution of carbon atoms in the unit cell of boron

0925-8388/92/$5.00

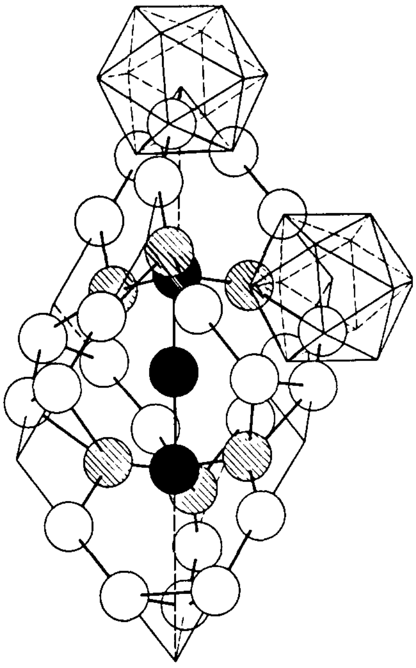

Fig. 1. Unit cell of boron carbide: ○, icosahedral boron atoms; ▨, equatorial boron atoms of the icosahedron bonding to the end atoms of the chain; ●, atoms of the three-atom chain (C–B–C or C–B–B) on the main diagonal of the unit cell, parallel to the *c* axis of the structure.

carbide is presented. It is based on the experimentally obtained phonon spectra in the range of the stretching mode of the three-atom chain and on suitable model calculations to fit the absorption and reflectivity spectra simultaneously.

2. Sample material and preparation

Specimens produced by different methods (Table 1) were provided by Elektroschmelzwerk Kempten (Kempten, FRG) an H. C. Starck (Laufenburg, FRG). A reliable characterization needs particularly a precise chemical analysis. Experience shows that the chemical composition of synthesized boron carbide, particularly in the case of hot pressing, deviates more or less substantially from the proportions of the ingredients, and so compositions as mentioned for example in ref. 19 can be regarded as not more than rough estimations.

For the present work the chemical analyses were performed on pieces of the specimens in the immediate neighbourhood of the investigated samples, and in the same laboratory (Elektroschmelzwerk Kempten) to exclude different methods of procedure. The method is described in ref. 20 and allows the separate determination of bonded and free carbon in boron carbide. In particular, some samples were at our disposal which had been used by Schwetz and Karduck [7] for the new determination of the carbon-rich limit of the homogeneity range of boron carbide. Their wet chemical and microprobe analyses let to the same results. Only in the case of the ^{10}B-enriched specimen was no analysis available, but the preparation was performed according to the standardized procedure for the carbon-rich limit composition, so that the composition $B_{4.3}C$ can be assumed in this case, too.

The sample surfaces were mechanically ground and carefully polished with diamond (finest grade, 1 μm) to avoid scattering of the light at the surfaces as far as possible. In some not completely dense samples the loss by scattering was corrected by a specially developed procedure [21].

3. Optical spectra

Reflectivity spectra of the samples were obtained with a Fourier transform IR spectrometer in the spectral range between 10 and 5000 cm^{-1} with a resolution of 2 cm^{-1}. By use of the Kramers–Kronig relation (KKR) the absorption spectra were calculated. Towards high frequencies the prerequisite for KKR was fulfilled, because the measurements were extended to the approximately dispersion-free range between absorption edge and lattice vibrations. Towards low energies there is no dispersion-free range in boron carbide because of the influence of the plasma edge on the optical properties [22, 23]. However, using a suitable extrapolation, which takes this semiconductor behaviour at low frequencies into account, the prerequisites for the allowable application of the KKR could be realized.

Characteristic reflectivity and absorption spectra (calculated by the KKR) of boron carbide are shown in Fig. 2 in comparison with the remeasured highly solvated spectra of the structurally related B_6O [24, 25]. The spectrum of B_6O essentially contains vibrations of the icosahedron only. Contrary to boron carbide, its arrangement of two oxygen atoms on the main diagonal of the unit cell has no IR-active valence vibration (stretching mode). Therefore the stretching mode ($E \| c$), which is object of the present investigation, is seen neither in the spectrum of B_6O nor in that of the single-crystal $B_{4.3}C$ sample with the investigated surface oriented closely perpendicular to the crystallographic *c* axis.

The difference between the absorption spectra of samples with different isotope enrichments is obvious. The change in the chemical composition as well leads to a distinctly different form of the absorption band, and moreover to a distinct frequency shift of the resonance curve (Fig. 3). Since the vibration mode under consideration is polarized parallel to c, for a quantitative comparison it must be ensured that the polycrystalline

TABLE 1. Samples and their properties

Designation	ESK 10	ESK 5	ESK 4	ESK 1	ST 43	ST 35	ST 15	ESK (I)
Producer	ESK	ESK	ESK	ESK	H.C. Starck	H.C. Starck	H.C. Starck	ESK
Nominal composition	$B_{2.4}C$	$B_{4.01}C$	$B_{4.23}C$	$B_{6.3}C$	$B_{7.91}C$	$B_{8.52}C$	$B_{10.37}C$	B_4C
B isotope distribution	Natural	Natural	Natural	Natural	Natural	Natural	Natural	92% ^{10}B
Preparation	Molten	Molten	Molten	Molten	Hot pressed	Hot pressed	Hot pressed and molten	Hot pressed
Chemical analysis (wt.%)								
B	68.26	78.22	79.19	83.10	84.00	82.0	88.7	ND
C (total)	31.57	21.65	20.78	14.65	11.8	10.7	9.5	ND
Impurities (ppm)								
O	1500	800	700	18200	26800	42000	1100	ND
N	1100	200	100	5100	9100	7400	13500	ND
Fe		<100	<100	<100	2900	19000	1100	ND
Mg		60 (typical)	60 (typical)	60 (typical)	1500	1600	10	ND
Al		<100	<100	<100				ND
Ca		<100	<100	<100				ND
Si		<1000	<1000	<1000				ND
Other metals	<2000	–	–	–	2100	3400	2400	ND
B:C ratio	4.3	4.3	4.3	6.30	7.91	8.52	10.37	4.3
(C bonded)	(4.20(12))	(4.34(12))						
C (at.%)	18.87	18.87	18.87	13.70	11.22	10.50	8.80	18.87

ESK, Elektroschmelzwerk Kempten; ND, not determined.

samples are randomly oriented. This is largely the case, because the size of the crystallites in the molten specimens is about 1 mm and in the hot-pressed samples less than 0.1 mm, and therefore the optical focus size of about 5 mm is sufficient to average the different crystallographic orientations. Excess carbon in boron carbide precipitates as graphite [1] and affects the spectrum of the matrix only by accordingly reducing the reflected signal. Therefore this error in the spectrum of sample $B_{2.4}C$ could be easily corrected.

In the spectral range close to the stretching vibration there are several small absorption bands, whose occurrence and strength are systematically related neither to the carbon content nor to a distinct impurity concentration.

4. Calculation model

Natural boron contains the isotopes ^{11}B (80.2%) and ^{10}B (19.8%). This means a mass difference of the vibrating atoms of 10% which, as already discussed in ref. 26, leads to a measurable shift of the phonon frequencies and to a modification of the form of the phonon absorption bands depending on the number of atoms vibrating. Quantitatively, according to the probability distribution of the isotopes on the boron sites in the structure a discrete distribution of the oscillator strengths on the single vibration frequencies must be expected. The analysis of the stretching mode of the central atom of the three-atom chain in boron carbide was based on these considerations. In addition to this frequency shift depending on the different masses of boron isotopes, the probable occupation of different sites by carbon atoms must be taken into account. Carbon consists of 99% of the isotope ^{12}C, and therefore a consideration of the isotope distribution is not necessary in this case. Thus it is obvious that the different arrangements of atoms in the three-atom chain of boron carbide (B–B–B, C–C–C, C–B–C, C–B–B, B–C–B), which can be assumed at first to be possible in principle, lead to different probability distributions of oscillator strengths of defined vibration frequencies, which make them distinguishable in the absorption and reflectivity spectra. For example, Fig. 4 shows the calculated probability distribution of the resonance frequencies of the C–B–C and the C–B–B chains in $B_{4.3}C$. It will be shown below that this chain combination has been proved to be the only applicable combination for boron carbide. The calculated probability distributions are immediately related to the experimentally obtained absorption spectra of the corresponding samples in Fig. 3.

Indeed, it is necessary to prove that the calculations can really be restricted to those three atomic sites. In particular, the essentially covalent bonds of the end atoms of the chain to the three adjacent equatorial atoms of the neighbouring icosahedra must be negligible, at least in a first approximation. These bonds are

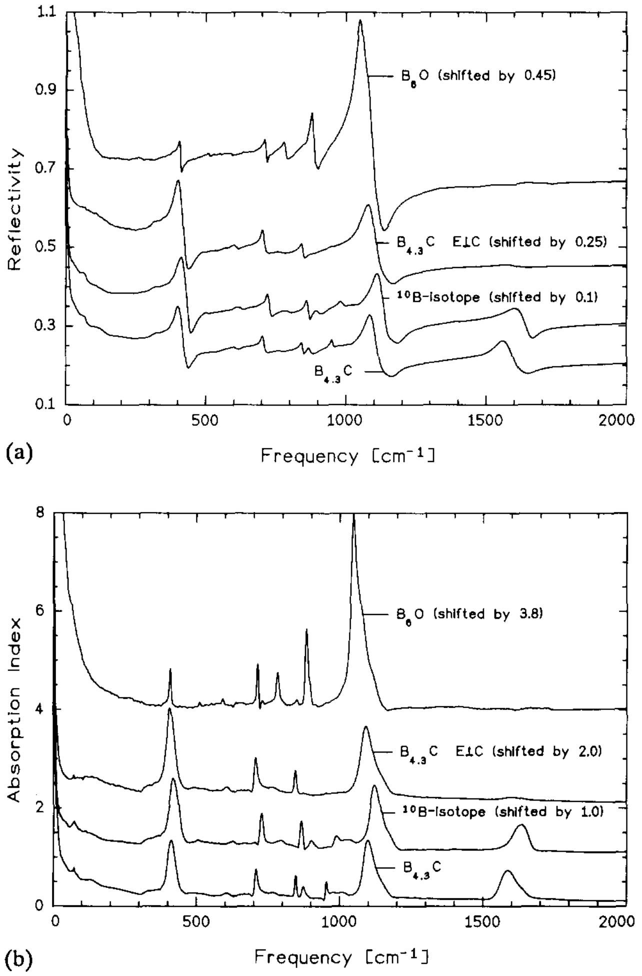

Fig. 2. Typical phonon spectra of boron carbide (160 K). (a) Reflectivity (measured). (b) Absorption index (calculated from the reflectivity by the KKR). The spectrum of B_6O (300 K) is included for comparison. The steep increase in reflectivity and absorption towards low energies is due to the strongly damped plasma vibrations.

arranged approximately in a plane, and the equatorial sites are occupied statistically by both boron isotopes and probably carbon atoms as well. The stretching vibration of the chain strains these bonds perpendicular to their orientation. It is known from the appropriately arranged molecules $^{11}BF_3$, $^{11}BCl_3$, and $^{11}BBr_3$ (see ref. 27 and references therein) that in these cases the restoring forces are less than 10% of the restoring forces of the valence vibrations. This can be assumed to be valid compared with the valence vibration of the chain as well, when the relation between restoring forces and distances of atoms belonging to the same row of the periodic table is considered [28], whose validity in the case of boron-rich solids was shown in ref. 29. Moreover, model fitting calculations including the equatorial atoms of the icosahedra proved to be unsatisfactory (Fig. 5).

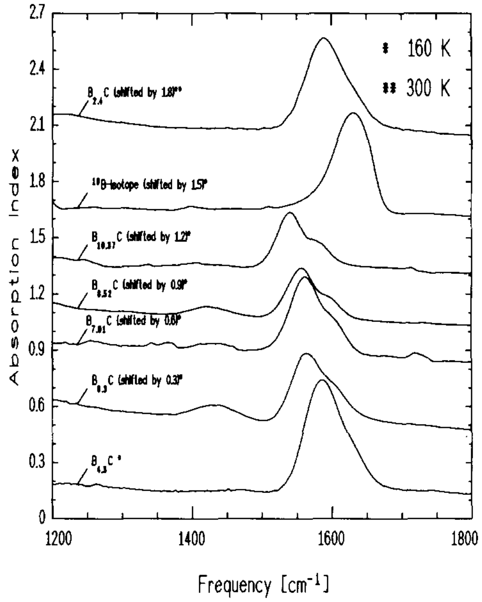

Fig. 3. Absorption spectra of the stretching mode of the three-atom chain in boron carbide for different chemical compositions and isotope enrichments.

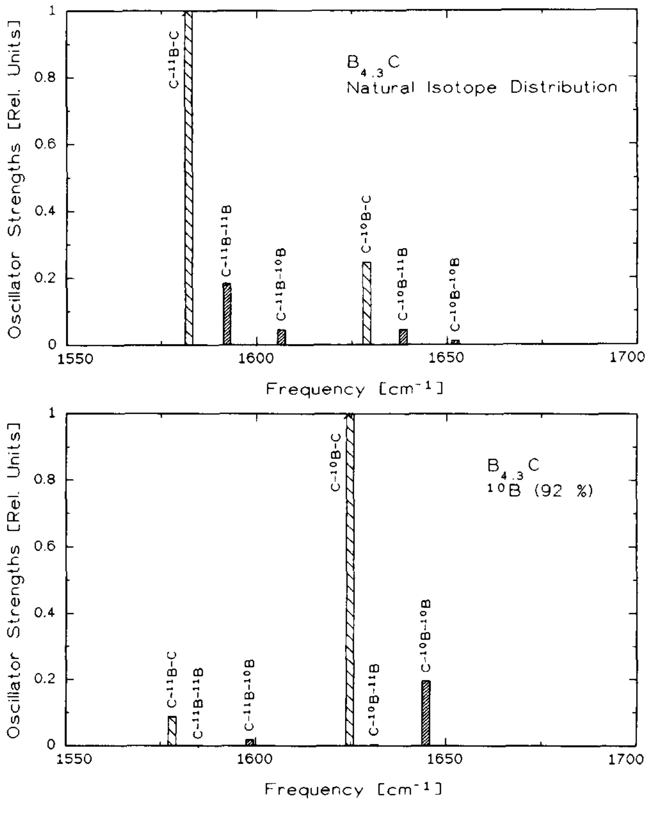

Fig. 4. Calculated relative probability distribution of the stretching vibration of the three-atom chain in $B_{4.3}C$ boron carbide (the absolute position in the spectrum was obtained from the adaptation of the measured spectra in Fig. 3): (a) $B_{4.3}C$ (natural isotope enrichment); (b) $B_{4.3}C$ (^{10}B, 92% enriched).

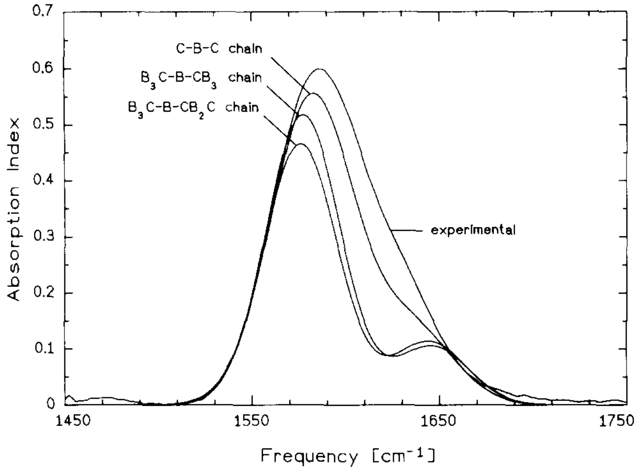

Fig. 5. Some test adaptations based on different bonding models of the end atoms of the three-atom chain. Even the best fit assuming a quasi-free C–B–C chain only proves not to be sufficient.

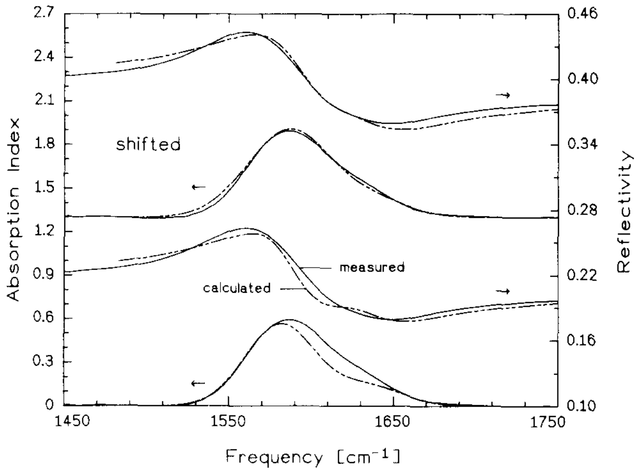

Fig. 6. Simultaneous adaptation to the IR spectra (absorption index and reflectivity) of the stretching mode of the three-atom chain: lower part C–B–C chains only; upper part, combination of C–B–C and C–B–B chains. Attention should be paid to the high precision of the measured reflectivity spectrum needed for reliable adaptations, particularly with respect to the absolute reflectivity.

However, when, according to the vibrations of a free linear XY_2 molecule, only the atoms of the chain were considered, the fitting calculations proved to be convincing, although only for the case that the combinations are restricted to C–B–C and C–B–B chains. Of course, only such fits were considered as physically meaningful which were based on low numbers of variables. For instance, Fig. 6 shows that the assumption of C–B–C chains only does not fit the experimental result, while the additional consideration of C–B–B chains leads to a satisfactory fitting. It is important to note that unambiguous results are only achievable when the absorption and the reflectivity spectra are fitted simultaneously. The damping of the phonons was taken into account by a gaussian distribution adapted to the experimental spectra. It was proved that possible small contributions of the Lorentz type can be neglected in our model calculations.

The results are consistent within the whole homogeneity range investigated and for the different isotope enrichments as well. For all B–C bonds and vibrations discussed the restoring force in the fits was kept unchanged for each specific composition; towards the boron-rich side the restoring force of the B–B bonds decreases. The damping was of the same order in all cases but differed slightly depending on the sample quality. For the ^{10}B in comparison with the ^{11}B isotope an isotope shift of 0.4% caused by the different zero-point energies had to be considered unchanged in the whole homogeneity range.

Hence, in the first approximation, apart from C–B–C and C–B–B, all the other chain compositions mentioned are largely to be excluded, and the same applies to the planar B_4 arrangement [8] as well. The error of this statement is less than about 5% related to the total number of unit cells.

5. Evaluation

The relative concentrations of the C–B–C and C–B–B chains obtained by a simultaneous fitting of the absorption spectra (Fig. 3) and the corresponding reflectivity spectra are presented in Fig. 7. While a monotonic decrease in the number of C–B–C chains and the corresponding increase in the number of C–B–B chains with decreasing carbon concentration is not surprising, the abrupt change in the relative chain concentrations between 14 and 10 at.% carbon is striking. To estimate the absolute contents of C–B–C and

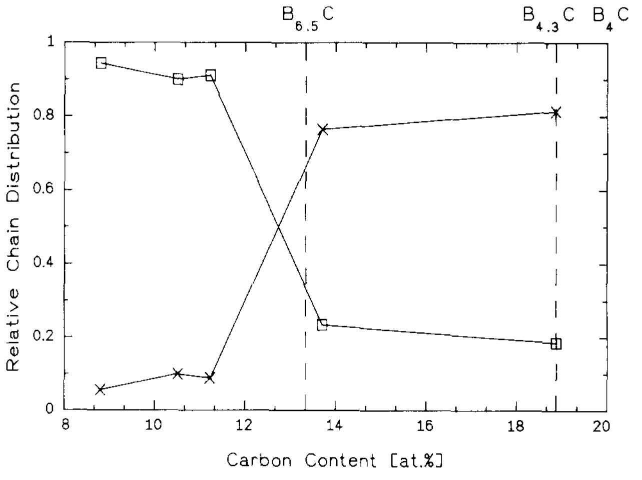

Fig. 7. Relative occurrence of C–B–C and C–B–B chains in the unit cells of boron carbide depending on the carbon content.

C–B–B chains in the structure, in Fig. 8 the integral oscillator strengths of the stretching vibration representing the sum of both types of chains is shown. On the basis of the qualified assumption that the stretching vibrations can be at least approximately considered as localized lattice vibrations, and taking the transition probability as constant, these integrals are proportional to the number of three-atom chains in the unit cells of boron carbide. Then it is obvious that a considerable proportion of unit cells increasing non-monotonically with decreasing carbon content contains neither C–B–C nor C–B–B chains. Also, the relative damping shown in Fig. 8 does not increase with decreasing carbon content. This justifies the model used of an approximately free stretching vibration of the three-atom chain, and makes it clear that the reduced oscillator strength is essentially not caused by strong damping processes in the boron-rich region of the homogeneity range.

On the basis of this evidence of unit cells without three-atom chains the remaining carbon atoms, which are assumed to substitute boron sites in the icosahedra, can be calculated using the chemical analysis data (Table 1). Two different models are considered.

(1) The unit cells without three-atom chains are *α* rhombohedral boron like, which means that there are no atoms saturating the three-centre bonds of the equatorial atoms of the icosahedra.

(2) Similarly to the boron halides, single boron atoms are positioned in the centre of a triangle of neighbouring atoms, here saturating the three-centre bonds of the equatorial atoms like the end atoms of the three-atom chain or the separate atoms in B_6O and homologous compounds [30].

It can be obtained from Fig. 9 that these two assumptions do not lead to significantly different carbon concentrations in the icosahedra. Therefore it is of minor importance that it cannot be decided from the present results which of the two assumptions is correct.

In Fig. 9 a third model is also included for comparison, namely the calculation for the case that, in contrast to the oscillator strengths obtained from experiment, decrease with decreasing carbon content, all the unit cells are completed by C–B–C or C–B–B chains in the proportion determined. However, such an assumption seems very improbable. The assumption that up to more than 50% of the material has a completely different structure seems improbable for different reasons, particularly because X-ray diffraction showed that the specimens investigated are largely single phase. Only in the most boron-rich compound were traces of *β* rhombohedral boron detectable [31]. The transition probability of the phonons could depend on the carbon content, and indeed the resonance frequencies of the C–B–C and C–B–B chains vary by about 3% within the homogeneity range (Fig. 10). However, this small shift seems merely to contradict the assumption that the transition probability is reduced by up to more than 50%, which would be necessary to explain the results this way. In particular, the results calculated according to the third model are not compatible with several specific composition-dependent properties of boron carbide.

On the basis of model 1, in Fig. 11 the variation in the relative concentrations of the different structural elements in the unit cell of boron carbide (B_{12} and $B_{11}C$ icosahedra, C–B–C and C–B–B chains) and of

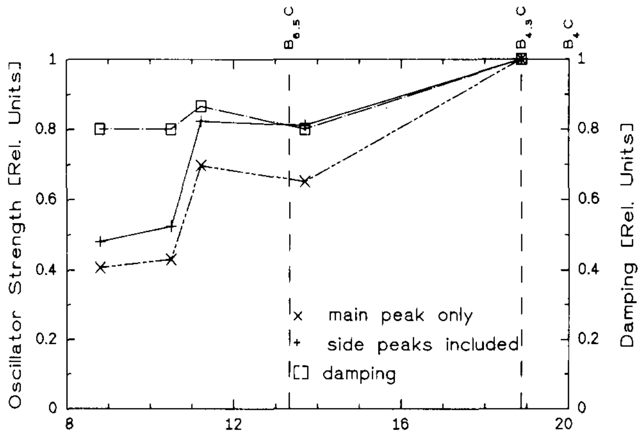

Fig. 8. Relative integral oscillator strengths of the stretching mode of the three-atom chains in boron carbide obtained by integrating the absorption bands in Fig. 3 and the damping constants used in these fits, related to the values obtained for $B_{4.3}C$.

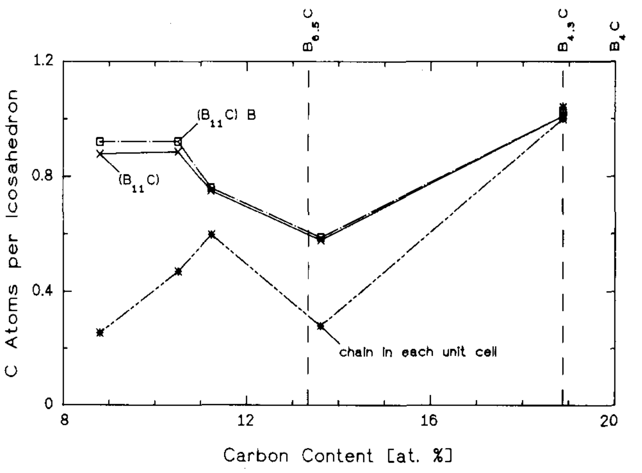

Fig. 9. Averaged number of carbon atoms per icosahedron for two structural models with and without boron atoms saturating the three-centre bonds of the equatorial atoms of the icosahedra. The lowest curve corresponds to the very improbable assumption that each unit cell of boron-rich boron carbide contains a three-atom chain (see text).

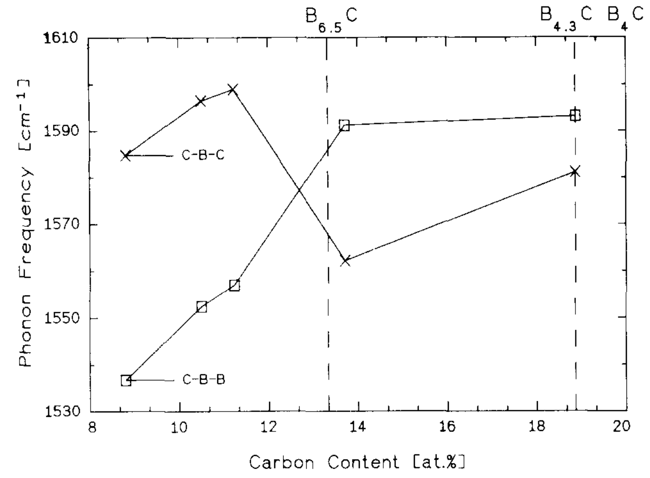

Fig. 10. Stretching mode resonance frequency of the C–B–C and C–B–B chains in boron carbide depending on the carbon content.

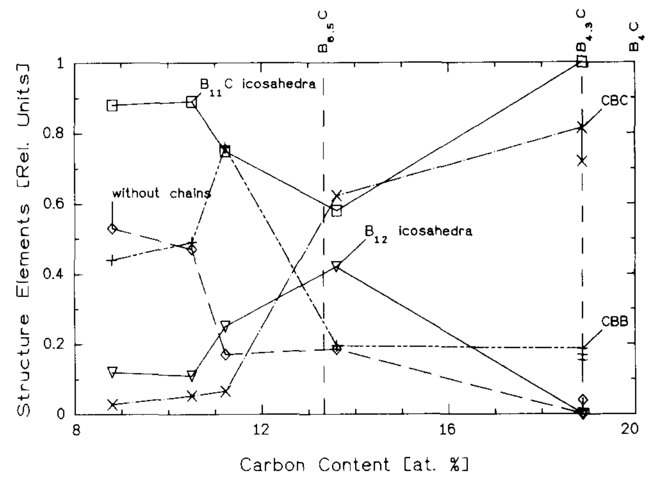

Fig. 11. Concentration of the structural elements (B_{12} and $B_{11}C$ icosahedra, C–B–C and C–B–B chains) in the rhombohedral unit cells and the proportion of chainless unit cells of boron carbide depending on the carbon content.

chainless unit cells throughout the homogeneity range are shown. Obviously the best-ordered region is that near the carbon-rich limit of the homogeneity range, and the region of highest disorder is the range between 12 and 14 at.% C. Near 11 at.% C there is a narrow region of relative order compared with the neighbouring composition regions. For the calculation of the force constants the $r_3((ny))$ frequency formula for linear XYZ molecules [27] was used with X = Z and f_{CB} for C–B–C respectively Y = Z and at first $f_{CB} \neq f_{BB}$ for C–B–B chains. The average $f_{C\text{-}B\text{-}B} = (f_{CB} + f_{BB})/2$ was verified by recalculating the experimental spectra successfully.

From the adaptation to the measured phonon spectra of $B_{4.3}C$ (Fig. 3) the force field constant of the C–B bond in the C–B–C chain was determined:

$$f = 0.56(1) \times 10^3 \text{ kg s}^{-1} = 5.6(1) \text{ mdyn Å}^{-1}$$

This value agrees quite well with $f = 5.4$ mdyn Å^{-1} theoretically calculated for the same problem by Abbott and Beckel [32], by applying a central force field model, and assuming C–B–C chains only. This B–C force constant was assumed to be valid in the C–B–B chain also, and the B–B force constant was calculated from the spectral shift of the corresponding resonance frequencies and was found to be the same. Hence in $B_{4.3}C$ the end atoms of the chains must be equally charged, independently of whether they are boron or carbon atoms. This can be taken as an experimental confirmation that from a carbon atom at the end position of the chain in $B_{4.3}C$ one electron more than from a corresponding boron atom is transferred to the icosahedron.

However, this does not hold in the more boron-rich structures of boron carbide. From the composition-dependent resonance frequencies of the C–B–C and C–B–B chains (Fig. 10) the force constants of the B–C and the B–B bonds were derived. For this calculation at first again the assumption was made that the C–B force constant is the same in C–B–C and C–B–B chains. However, this assumption yielded distinctly lower force constants for the C–B bond (Fig. 12). Therefore the real force constant in the C–B–B chains corresponds to the average of the B–C and B–B values in Fig. 12. From $B_{4.3}C$ to $B_{6.5}$ it is largely independent of the carbon content, and then decreases linearly as the carbon content decreases further. The validity of the presumed linear force law was checked by calculating the spectral shift between the resonance frequencies of both types of chains: they proved to agree exactly

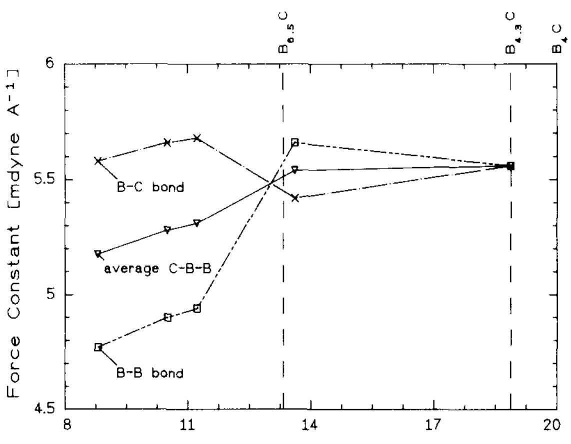

Fig. 12. Force constants of the B–C and B–B bonds in the three-atom chains of boron carbide. The curve labelled "B–B bond" is only an interim result in the calculation. It is based on the assumption that the B–C force constants are the same in C–B–C and C–B–B chains, which is only fulfilled in $B_{4.3}C$ (see text). The curve labelled "average C–B–B" represents the real force constant obtained for the C–B–B chains (average of B–C bond and B–B bond).

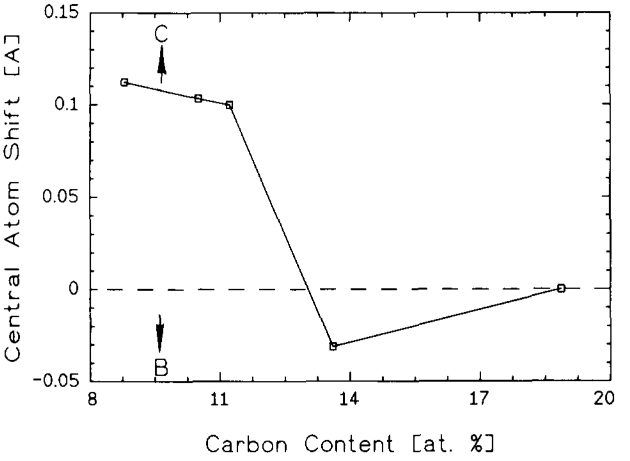

Fig. 13. Shift of the central atom of the C–B–B chain depending on the unsymmetric force constant at different carbon contents. Absolute values calculated related to the B–C distance in $B_{4.3}C$ [33].

with the data obtained from the empirically fitted spectra.

Hence, contrary to $B_{4.3}C$, in the boron-rich boron carbides the end atoms of the C–B–B chains are differently charged, which leads to a shift of the central boron atom from the central position into the direction of the higher force constant. The C–B force constant of the C–B–C chain was again assumed to be valid in the C–B–B chain as well, and this shift was calculated (Fig. 13). At higher carbon contents in the homogeneity range the central atom is slightly shifted towards the boron atom. This shift changes its sign close to $B_{6.5}C$, and with the approach to the boron-rich limit the bond length change amounts to about 0.11 Å, *i.e.* about 8% of the B–C bond length of 1.436 Å within the chain of $B_{4.3}C$ [33].

6. Discussion

The results of this work require that the present ideas of the structure of boron carbide and its change within the homogeneity range are to be revised. Neither the structure $(B_{11}C)C$–B–C of the chemical composition B_4C at the carbon-rich limit of the homogeneity range nor $(B_{12})C$–B–C, the structure of $B_{6.5}C$, which has been assumed by a number of researchers to be the really ideal structure of boron carbide, exists as a uniform crystal structure. Until now it has generally been accepted that with decreasing carbon content the modification of the boron carbide structure can be described by a statistical exchange of $B_{11}C$ by B_{12} icosahedra and of C–B–C by C–B–B chains; this is disproved by the present results, too.

In reality, nowhere in the homogeneity range is the structure uniform; rather it consists of mixtures of B_{12} and $B_{11}C$ icosahedra at the vertices, and of mixtures of C–B–C and C–B–B chains on the principal diagonal of the rhombohedral unit cells. Moreover, particularly with decreasing carbon content a growing proportion of unit cells without three-atom chains develops, whose concentration exceeds even 50% at carbon contents lower than about 9 at.%. Throughout the homogeneity range complicated vagaries of these structural elements determine the actual structures. Apparently in the case of boron carbide a completely homogeneous structure is not the energetically most favourable state. This is in accordance with the recent observation of Schwetz and Karduck [7] that the carbon-rich limit composition is not the simple composition B_4 but $B_{4.3}C$. This is additionally supported by the asymptotic approach of the C–B–B chain concentration to the carbon-rich limit of the homogeneity range.

These new results on the one hand explain easily the dependence of several properties of boron carbide on the chemical composition, while on the other hand they disprove some essential assumptions used until now in certain models for the interpretation of properties.

A qualitative criterion of the long-range order of the structure is the degree of distinctness of the lattice vibration bands of the icosahedron in the IR spectrum. The present results confirm the experience obtained from these spectra that the distortions are lowest near the carbon-rich limit of the homogeneity range. However, at first it was surprising that the spectrum of $B_{7.91}C$ is more distinct than those of the samples adjacent in composition [34]. Figure 11 explains this immediately: at 11 at.% C there is a very narrow range of higher order in comparison with the adjacent compositions.

Several researchers [35–39] assumed the composition $B_{6.5}C$ (structural formula, $(B_{12})C$–B–C) to be the ideal and therefore the best with which to make representative conclusions. The present results show that this is not at all the case. In reality this composition is close to the least-defined structure in the homogeneity range of boron carbide. Therefore the conclusions based on this structural model have only a limited validity.

The variation in the lattice constants with decreasing carbon content cannot be attributed simply to the increasing number of B_{12} icosahedra only. The re-increasing number and influence of $B_{11}C$ icosahedra at carbon contents lower than about 13.5 at.% is obviously compensated by the increasing number of chainless unit cells. In the region close to the boron-rich limit of the homogeneity range a significant proportion of the chains, which contribute considerably to the stabilization of the boron carbide structure near the carbon-rich limit, is missing. Instead obviously the more stable $B_{11}C$ icosahedra are needed to stabilize the structure. This stabilization of the icosahedron by the substitution of a boron atom by carbon is known from theoretical calculations [16, 17] and from investigations on carbon-doped β rhombohedral boron [15], and it is in accordance with the Jahn–Teller effect [13] as well.

From empirical industrial experience it results that the maximum hardness of boron carbide is realized at the carbon-rich limit of the homogeneity range and decreases with decreasing carbon content. This has been attributed to the decreasing lattice constant. However, Fig. 11 shows that at this composition the most homogeneous structure within the whole homogeneity range exists, and hence the microscopic stresses in the structure are the lowest. This may be a more relevant explanation for the hardness behaviour of boron carbide.

The thermal conductivity of boron carbide decreases abruptly when the composition is changed from B_4C to $B_{6.5}C$. This was attributed to the redistribution of the carbon atoms in the structure, particularly within the icosahedra; carbon atoms at the end positions of the chain are expected to bond preferably to boron atoms on equatorial sites, while boron atoms at the end positions prefer carbon atoms as bonding partners [34, 40]. From Fig. 11 it results that much stronger structural distortions are the real reason. Within this rather small range of chemical compositions the structure changes from the most homogeneous to the most distorted.

Towards the boron-rich limit of the homogeneity range the thermal conductivity of boron carbide increases slightly [41]. This is in accordance with the results in Fig. 11 as well, showing that a certain kind of lower order is developing because the $B_{11}C$ icosahedra are being preferred, while unit cells with C–B–B chains and such without chains are both close to 50%, keeping the structure distorted to a considerable degree.

The acoustic velocity in boron carbide is quite large, consistent with light atoms and stiff bonds [42]. It decreases slightly from the carbon-rich limit to about 13 at% C content and rapidly with a further decrease in the carbon content. When the force constant of the stretching mode of the central atom in the majority chains (Fig. 12) is taken as a criterion of the bond strength of the whole structure, an immediate correlation with the acoustic velocity varying as $\sqrt{f_{CBB}}$ is evident.

In the carbon-rich part of the homogeneity range the resonance frequency of the dominating C–B–C chains (and of the C–B–B chain as well) decreases slightly, while towards the boron-rich limit the resonance frequency of the preferred C–B–B chains decreases considerably. The reverse trend of the minority C–B–C chain resonance in the transition range emphasizes the local stresses in the structure, since the influence on the largely freely vibrating stretching mode of the three atom chain can be assumed to come particularly from the immediate neighbourhood and not from the averaged influence of the total structure.

The results of the present paper yield a new argument [43] against a basic assumption in Emin's theory on the electronic transport in boron carbide [44]. He attributes the carrier transport to the hopping of bipolarons between $B_{11}C$ icosahedra. However, the maximum conductivity in boron carbide is at about the composition B_7C [4, 45, 46], which, according to Fig. 9, is close to the minimum concentration of $B_{11}C$ icosahedra in the structure.

Acknowledgments

Parts of the results were obtained within a project supported by the Minister of Research and Technology of the FRG under Contract 317-4003-0328845A. The authors are indebted to D. Fister and H. Neisius, H. C. Starck, Laufenburg, FRG, for providing several of the boron-rich boron carbide specimens for these investigations.

References

1 K. A. Schwetz and A. Lipp, Boron carbide, boron nitride, and metal borides. In *Ullmann's Encyclopedia of Industrial Chemistry,* Verlag Chemie, Weinheim, 1985, p. 295.
2 F. Thévenot, Sintering of boron carbide and boron-carbide–silicon-carbide two-phase materials and their properties. In H. Werheit (ed.), *Proc. IX Int. Symp. on Boron, Borides, and Related Compounds, Duisburg,* University of Duisburg, 1987, p. 246.
3 C. Wood, The transport properties of boron carbide prepared by different techniques. In H. Werheit (ed.), *Proc. IX Symp. on Boron, Borides, and Related Compounds, Duisburg,* University of Duisburg, 1987, p. 213.
4 H. Werheit and U. Kuhlmann, *Proc. Int. Conf. on Powder Metallurgy, Kiev, 1991* to be published.
5 H. Werheit, Boron compounds. In O. Madelung, M. Schulz and H. Weiss (eds.), *Landoldt–Börnstein, Numerical Data and Functional Relationships in Science and Technology, New Series, Group III Semiconductors,* Vol. 17g, Springer, Berlin, 1984, p. 9.
6 C. Wood, Electronic transport in boron carbide, *AIP Conf. Proc., 140* (1985) 206.
7 K. A. Schwetz and P. Karduck, Investigations in the boron–carbon system with the aid of electron probe microanalysis, *AIP Conf. Proc., 231* (1990) 405.
8 H. L. Yakel, *Acta Crystallogr. B, 31* (1975) 1797.
9 P. J. Bray, NMR studies of borates and borides, *A.I.P. Conf. Proc., 140* (1985) 142.
10 M. N. Alexander, Nuclear magnetic resonance studies of the structure of boron carbides, *A.I.P. Conf. Proc., 140* (1985) 168.
11 T. M. Duncan, The distribution of carbon in boron carbides: ^{13}C nuclear magnetic resonance studies, *A.I.P. Conf. Proc., 140* (1985) 177.
12 R. J. Kirkpatrick, T. Aselage, B. L. Phillips and B. Montez, ^{11}B and ^{13}C NMR spectroscopy of boron carbides, *AIP Conf. Proc., 231* (1990) 261.
13 R. Franz and H. Werheit, *Europhys. Lett., 9* (1989) 145.

14 R. Franz and H. Werheit, Influence of the Jahn–Teller effect on the electronic band structure of boron-rich solids, *AIP Conf. Proc., 231* (1990) 29.

15 H. Werheit, M. Laux, U. Kuhlmann and T. Lundström, to be published.

16 M. M. Florence and C. L. Beckel, Electronic studies of B_4C, *AIP Conf. Proc., 231* (1990) 37.

17 L. Kleinman, *Ab initio* calculations of boron and its carbides, *AIP Conf. Proc., 231* (1990) 13.

18 D. M. Bylander and L. Kleinman, *Phys. Rev. B, 42* (1990) 1394.

19 D. R. Talland, T. L. Aselage, A. N. Campbell and D. Emin, *Phys. Rev. B, 40* (1989) 5649.

20 K. A. Schwetz and J. Hassler, *J. Less-Common Met., 117* (1986) 7.

21 U. Kuhlmann and H. Werheit, *Bruker News,* to be published.

22 H. Binnenbruck and H. Werheit, *Z. Naturforsch., Teil A, 34* (1979) 787.

23 H. Werheit, Optical properties of boron-rich solids with icosahedral structure. In R. Freer (ed.), *The Physics and Chemistry of Carbides, Nitrides and Borides,* Kluwer, Dordrecht, 1990, p. 705.

24 H. Werheit, Optical characterization of icosahedral boron modifications and compounds, *Progr. Cryst. Growth Charact., 16* (1988) 179.

25 H. Werheit and H. Haupt, *Z. Naturforsch., Teil A, 42* (1987) 925.

26 H. Werheit, U. Kuhlmann, N. E. Solov'ev, G. P. Tsiskarishvili and G. V. Tsagareishvili, Optical properties of α-rhombohedral boron, *AIP Conf. Proc., 231* (1990) 350.

27 G. Herzberg, *Molecular Spectra and Molecular Structure, II. Infrared and Raman Spectra of Polyatomic Molecules,* van Nostrand Reinhold, New York, 1946, p. 178.

28 J. Waser and L. Pauling, *J. Chem. Phys., 18* (1950) 747.

29 H. Werheit and H. Haupt, On the phonon spectra of boron carbide and β-rhombohedral boron, *AIP Conf. Proc., 231* (1990) 355.

30 T. Lundström, Structural aspects of some boron-rich refractory compounds related to B_4C, *AIP Conf. Proc., 231* (1990) 186.

31 T. Lundström, personal communication (1991).

32 B. S. Abbott and C. L. Beckel, Vibrational analysis of B_4C, *AIP Conf. Proc., 231* (1990) 344.

33 B. Morosin, A. W. Mullendore, D. Emin and G. A. Slack, Rhombohedral crystal structure of compounds containing boron-rich icosahedra, *AIP Conf. Proc., 140* (1985) 70.

34 P. A. Medwick, D. G. Cahill, A. K. Raychaudhuri and R. O. Pohl, Specific heat and thermal conductivity of amorphous boron, *AIP Conf. Proc., 231* (1990) 363.

35 M. Bouchacourt and F. Thevénot, *J. Less-Common Met., 82* (1981) 227.

36 G. Will and K. H. Kossobutzki, *J. Less-Common Met., 44* (1976) 87.

37 D. R. Armstrong, J. Bolland, P. G. Perkins, G. Will and A. Kirfel, *Acta Crystallogr. B, 39* (1983) 324.

38 D. W. Bullett, Further electronic structure studies of boron and boron-rich borides. In R. Freer (ed.), *The Physics and Chemistry of Carbides, Nitrides and Borides,* Kluwer, Dordrecht, 1990, p. 513.

39 A. C. Switendick, The electronic structure of crystalline boron carbide I: B_{12} icosahedra and C–B–C chains. In R. Freer (ed.), *The Physics and Chemistry of Carbides, Nitrides and Borides,* Kluwer, Dordrecht, 1990, p. 525.

40 P. R. H. Türkes, E. T. Swartz and R. O. Pohl, Thermal properties of boron and boron carbides, *AIP Conf. Proc., 140* (1985) 346.

41 H. Werheit and U. Kuhlmann, to be published.

42 T. L. Aselage, D. R. Tallant, J. H. Gieske, S. B. van Deusen and R. G. Tissot, Preparation and properties of icosahedral borides. In R. Freer (ed.), *The Physics and Chemistry of Carbides, Nitrides and Borides,* Kluwer, Dordrecht, 1990, p. 97.

43 H. Werheit, On the electronic transport properties of boron carbide. In R. Freer (ed.), *The Physics and Chemistry of Carbides, Nitrides and Borides,* Kluwer, Dordrecht, 1990, p. 677.

44 D. Emin, Electronic and vibrational hopping transport in boron carbides, *AIP Conf. Proc., 231* (1990) 65.

45 H. Werheit and K. de Groot, *Phys. Status Solidi, 97* (1980) 229.

46 H. Werheit, K. de Groot, W. Malkemper and T. Lundström, *J. Less-Common Met., 82* (1981) 153.